New Journal of Physics

The open−access journal for physics

Resonant transmission of microwaves through a finite length subwavelength metallic slit

J R Suckling[1,3]**, A P Hibbins**[1]**, J R Sambles**[1] **and C R Lawrence**[2]

[1] School of Physics, Exeter University, Devon EX4 4QL, UK
[2] QinetiQ, Cody Technology Park, Farnborough GU14 0LX, UK
E-mail: J.R.Suckling@ex.ac.uk

Abstract. The resonant transmission of microwaves polarized perpendicular to a single subwavelength slit of finite length is presented in detail. It is shown that the resonant frequency rises monotonically as slit length is reduced. Increasing confinement of the resonant fields within the slit is shown to cause the frequency rise. Angle dependence of the transmission is also presented. The results show clearly Fabry-Perot-like standing waves in the direction of propagation with waveguide mode behaviour in the orthogonal direction.

Contents

[3] Author to whom any correspondence should be addressed.

1. Introduction

Ever since Ebbesen *et al* [1] first published their remarkable evidence of high-intensity light transmission through arrays of subwavelength circular apertures in metal films, there has been great interest in resonant transmission phenomena. The initial results were attributed to the resonant coupling of photons into surface plasmons polaritons (SPPs) on the incident surface. The SPPs then couple from the top interface through to the bottom interface of the array, massively enhancing the transmission over that which might be expected if single apertures in isolation were considered [2]. Although they are clearly not the same as holes, because of the boundary conditions, arrays of parallel sided slits in thick (>wavelength) metal substrates have also been explored theoretically, seemingly as an analogy to the hole array [3]. It was shown that SPPs again provide a transmission channel through such a grating. In addition it was found that Fabry-Perot like modes are formed within each slit of the grating mediating strongly resonant transmission [4]–[6]. The presence of these transverse electric (TE, E-fields normal to the slit walls) Fabry-Perot modes defines the major, and very significant, difference between slits and small holes in a metal film. Electric fields are constrained to the normal of the surface of a perfect metal and are similarly approximately constrained in a real metal. For this to be the case in a circular hole, the linearly polarized incident radiation will need to excite a resonant mode which has at least two nodes around the circumference of the hole. Thus unless the holes are large enough for the wavelength to be of order of hole circumference, a hole will not support the Fabry-Perot type modes supported by a slit. Likewise, this boundary condition will prevent transmission of photons through a subwavelength slit if the incident photons are polarized parallel to the slit. The resonant transmission of perpendicularly polarized photons through slit gratings at microwave frequencies has been experimentally demonstrated with the grating structures acting like a Fabry-Perot interferometer with non-perfectly reflecting mirrors [7]. There is of course no need to have an array of slits to show this behaviour. Work into the transmission of infinitely long subwavelength slits has been reduced to the case of just a single isolated slit in a metal plate, both theoretically [8] and experimentally [9, 10]. It has been found that the resonant frequency is dependent on both the separation of the metal plates and the conductivity of the metal in which the slit is formed.

Likewise the enhanced optical transmission through the hole arrays had naturally led to the investigation of the individual elements of the array. Although this has been studied theoretically by Bethe [2], only limited experimental study of single holes on optical scales had been possible prior to the advent of nano-manufacturing techniques, e.g. focused ion beam lithography. The transmission of a single subwavelength hole in a thin metal film has now been studied in the optical regime [11]. Very recently this has been extended theoretically to consider the transmission of photons through a rectangular aperture, whose dimensions are of the order of the incident wavelength, in thin metal film [12]. It was shown that resonant transmission occurred at wavelengths similar to those predicted by waveguide theory [13].

The work presented here is the experimental investigation of the transmission of microwaves through a single subwavelength slit of finite length, in metal the depth of which is of the order of the incident photon wavelength. This represents a cross-over between the works presented in [9, 13] and shows how the resonant frequencies of slits are affected by the presence of metallic walls at the ends of the slit.

Reference [13] discusses transmission of a rectangular hole and makes the analogy of a similarly shaped waveguide. In microwave theory rectangular waveguides are considered as an

open aperture into a tube which extends to infinity along the *z*-axis. The sides of the openings along the *x*- and *y*-axes are assigned lengths *l* and *w* respectively, such that $l > w$. Given that the walls of the waveguide are perfectly conducting, considered a good approximation of a metal in the microwave regime, it is easily shown that only certain frequencies of photons will be allowed to propagate, given by:

$$f = \frac{c}{2\pi}\left[\left(\frac{M\pi}{l}\right)^2 + \left(\frac{P\pi}{w}\right)^2\right]^{1/2}, \tag{1}$$

where *M* and *P* are the resonant order along *l* and *w* respectively. The allowed propagating modes are thereby simply defined by the dimensions of the waveguide entrance. The allowed propagating modes within a rectangular waveguide are divided into two categories, TE and TM modes. TE modes are defined as containing no electric field components parallel to the axis of propagation; TM modes contain no magnetic components along this axis.

In contrast to the rectangular waveguide, the simple Fabry-Perot interferometer places no restriction on the frequency of photons that can enter it, but will only support certain resonant modes between two parallel perfectly reflecting mirrors separated by distance, *t*, at frequencies defined by:

$$f = \frac{cN}{2t}, \tag{2}$$

where *N* is the mode number. A single subwavelength slit ($w \ll \lambda$) will resonate for radiation polarized across the slit at similar frequencies, where *t* defines the depth of the slit and not the plate separation. (However, this approximation is only valid for an infinitely long slit in perfect metal when the slit width is almost zero ($w \to 0$).) In reality, the resonant frequency of any mode is always slightly lower than this prediction. This is due to two factors; when the slit is wide ($w > 70\,\mu$m) the resonant frequency reduces due to the boundary conditions at the open ends of the slit [8, 10] and for a narrow slit ($w < 70\,\mu$m) the penetration of fields into the metal means the resonant fields sample the inevitably finite conductivity, again reducing the resonant frequency [10].

A finite length waveguide might be expected to allow propagating modes that satisfy the requirements of both the entrance aperture (waveguiding) and depth of the slit (Fabry-Perot character). As we are interested in the allowed propagating modes of a slit, which is subwavelength along $w(w \ll \lambda)$, it can be shown from standard microwave waveguide theory that only the TE mode will be allowed to propagate, such that $P = 0$. Therefore, it might be expected that hat a single finite length slit in deep metal plate will only resonate at frequencies approximated by:

$$f_{N,M} = \frac{c}{2\pi}\left[\left(\frac{N\pi}{t}\right)^2 + \left(\frac{M\pi}{l}\right)^2\right]^{1/2}. \tag{3}$$

The work presented here will test the transition from an infinitely long single subwavelength slit into a singular small aperture, approaching the limit of a true subwavelength element in the remarkable hole arrays. The experimental setup for studying the finite length slit
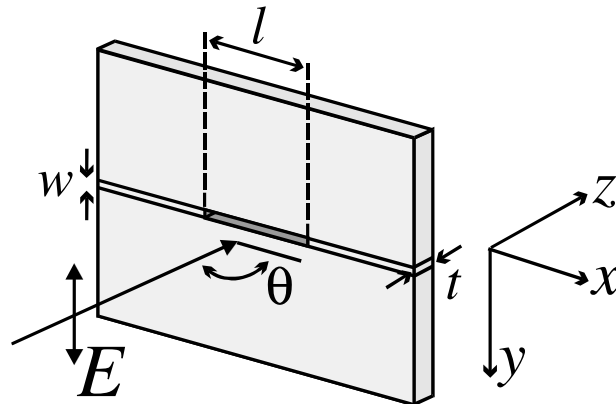
Figure 1. Experimental setup with dimensions, microwave polarization and axes labelled. Axes chosen to correspond to the computer model.

(figure 1) consists of two large aluminium plates of face area $200 \times 400\,\text{mm}^2$ and thickness 19.58 mm separated by smooth $80\,\mu\text{m}$ aluminium foil spacers. This slit width is chosen such that perturbations on the Fabry-Perot prediction from the open ends of the slit and the finite conductance of the metal are minimized. The metal spacers can be moved along between the plates thereby defining the length of the slit. The slit is aligned horizontally and placed directly between two microwave horns, one acting as a source, the other as a detector, orientated so that the microwaves are polarized perpendicular to the slit. The detector horn is placed at a distance of $\sim$15 cm from the metal plate, close enough to give the best possible signal from very short slits, yet far enough away not to be considered near-field. The microwave generating apparatus used is a Hewlett-Packard 8350B sweep oscillator connected to an Agilent 8757D scalar network analyser. Intensity data is recorded automatically by a computer as a function of angle and frequency. Frequencies used are over the range $40 < f < 60\,\text{GHz}\,(5 < \lambda < 7.5\,\text{mm})$ and the plates are rotated in the x–y-plane by up to $\pm 40°$. Given the polarization and plane of rotation of the sample, the microwaves are always s-polarized (TE).

To explore the fields within the experimental sample at resonance, it is recreated within Ansoft's high frequency structure simulator (HFSS; Ansoft Corporation, Pittsburg, USA). This program uses the finite element method (FEM), whereby the model is divided into many tetrahedra over which Maxwell's equations may be solved to reproduce the electromagnetic response of the experimental sample. The orientation of the axes marked in figure 1 corresponds to that used within the modelling program and therefore with subsequent field profiles shown within this work.

2. Results and discussion

2.1. Normal incidence resonant response of the slit

To explore the change in the resonant frequency of the slit as a function of slit length, the foil spacers are moved over the length range $18 < l < 200\,\text{mm}$. The experimental data is plotted in figure 2 as a function of f^2 versus $1/l^2$ (open circles). Also plotted is the prediction of equation (3) (dashed line) and that of the FEM model (solid line).
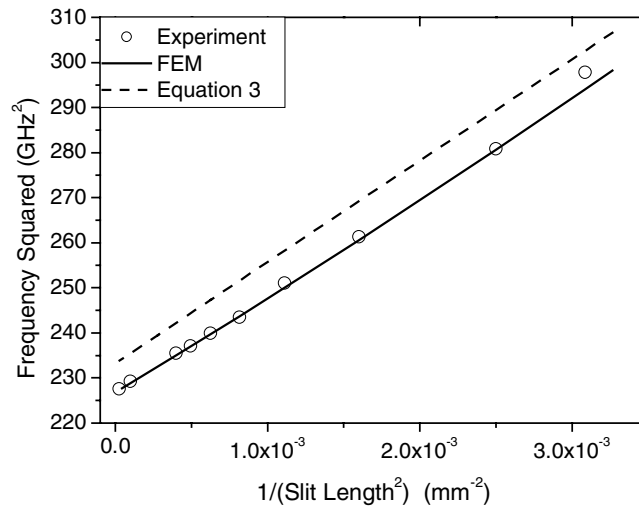
Figure 2. Experimental data, square of resonant frequency against square of inverse slit length, $18 < l < 200$ mm for a slit width, $w = 80\,\mu$m (○). FEM prediction (———) and equation (3) prediction (– – – – –).

A linear monotonic increase in frequency is demonstrated, beginning at the resonant frequency of an infinitely long single slit and rising until a slit length roughly corresponding to the wavelength of the incident microwaves has been reached. At this slit length the signal becomes too weak to measure accurately (this is not the cut off limit of the waveguide, which is of course $l \sim \lambda/2$, but an issue of signal to noise). The prediction of the simple equation (3) is shown to lie above the experimental, this is not unexpected as the $80\,\mu$m slit width will make the resonant frequency reduce as has been discussed. Importantly, the trends of this simple theory and the data agree, proving that the finite length slit resonates in the same manner as an infinitely long slit, but perturbation by the presence of the metal spacers forces the frequency to rise. The FEM model is shown to agree very well with the data. Figure 3 shows the time-averaged electric field within the slit. It can be seen from the positions of the field maxima that this is the $N = 2, M = 1$ mode for a slit of length 25 mm. The resonant field profiles along the two axes are clearly visible.

The first feature of figure 3 to note is the large enhancement of the internal resonant fields over that of the incident wave magnitude. Within HFSS the injected incident beam has an electric component magnitude of $1\,\mathrm{V\,m^{-1}}$, thus the figure indicates an enhancement of ~ 80. Secondly, it is also interesting to note that figure 3 neatly demonstrates the difference in the two sets of boundary conditions at the ends and sides of the slit and their effect on the position of the nodes of the resonant fields. Firstly, the open end slit Fabry-Perot-type resonance is illustrated along the z-axis. These are characterized by electric field maxima at the openings that rapidly decay in a distance that is $\ll \lambda$ outside the slit. Hence the end of the resonant electric field profile is approximately an anti-node. Secondly, the boundary condition of a closed-end Fabry-Perot resonator is shown along the x-axis. In this instance the tangential component of the electric field, with respect to the metal surface, is reduced to zero and therefore the overall electric field at the metal surface becomes zero giving a node.

Within a resonant cavity such as a single slit, the resonant electric and magnetic fields are both temporally and spatially $90°$ out of phase. Figure 4 shows the time-averaged magnetic fields
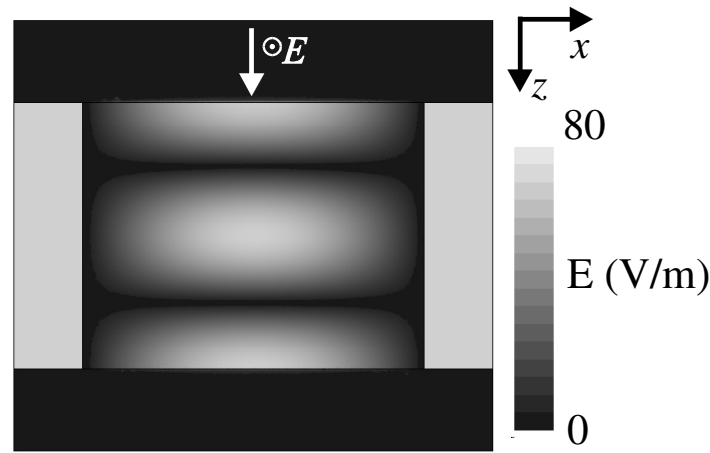
Figure 3. Time-averaged electric field magnitude within slit $l = 25\,\text{mm}$, $w = 80\,\mu\text{m}$ and $t = 19.58\,\text{mm}$. Resonant mode $N = 2, M = 1$ is shown. Incident microwave beam and coordinate axes are shown, corresponding to computer model. Incident electric field magnitude $= 1\,\text{V m}^{-1}$.
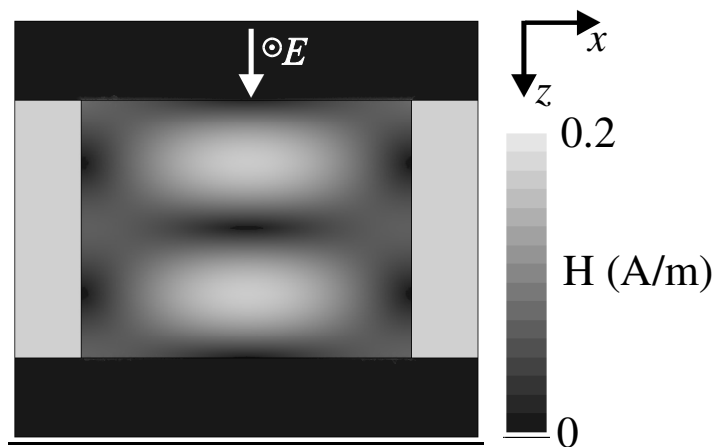

Figure 4. Time-averaged magnetic field magnitude within a slit of $l = 25\,\text{mm}$, $w = 80\,\mu\text{m}$ and $t = 19.58\,\text{mm}$. Resonant mode $N = 2, M = 1$ is shown. Incident microwave beam and coordinate axes are shown, corresponding to the computer model. Incident electric field magnitude $= 0.0027\,\text{A m}^{-1}$.

of the $N = 2$, $M = 1$ mode. The conditions in the middle of the slit show that the magnetic and electric fields (figure 3) are indeed $90°$ out of phase along the z-axis along the centre of the slit. The same is not true for the vertical edges of the slit where the magnetic field, like the electric field, is shown to be weak. In this region, the flow of the surface currents along the inside of the slit is disrupted sufficiently by the slit geometry to prevent the formation of strong fields, magnetic or electric. As HFSS injects a magnetic field of magnitude $0.0027\,\text{A m}^{-1}$ (defined by $H = E/(\mu_0 c)$), a magnitude of $0.2\,\text{A m}^{-1}$ within the slit shows again an enhancement of ~ 80.

It should be noted that only transmission of photons polarized perpendicular to the slit has been discussed. Such photons cannot propagate when the slit width is less than $\sim\lambda/2$. Of course
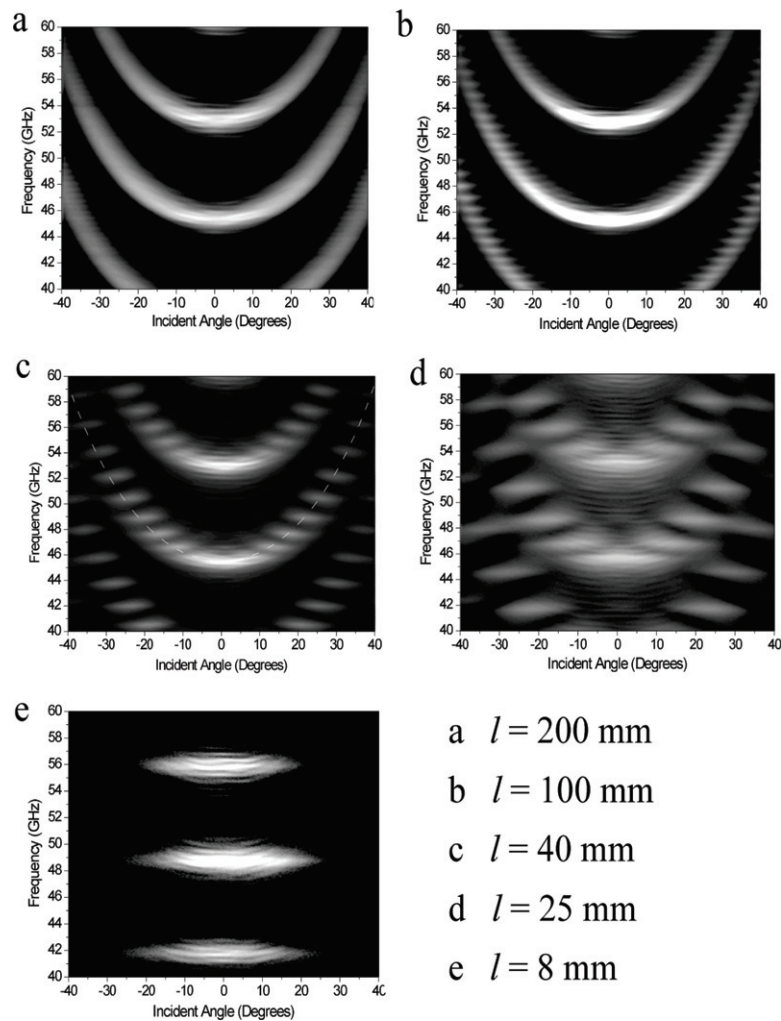
Figure 5. Experimental data showing resonant transmission of a finite length single slit as a function of slit length. Transmission intensity of slit lengths (a) 200 mm, (b) 100 mm, (c) 50 mm, (d) 40 mm and (e) 8 mm shown are plotted over frequency range $40 < f < 60$ GHz and angle range $-40 < \theta < +40°$. Light areas indicate strong transmission.

when the photons are polarized along the slit there can be no propagation for the very narrow slits considered here ($\ll\lambda$).

2.2. Off normal incidence resonant response of the slit

In the previous section, only the $M = 1$ mode can be readily coupled to as the phase conditions at the ends of the slit along the *x*-axis are such that only symmetric modes may exist. Anti-symmetric modes, in which fields at opposite ends of the slit are 180° out of phase, can only be coupled to by a beam with a higher angle of incidence in order to give the correct phase conditions. From equation (3), it is expected that the higher-order resonant modes along the length of the slit will resonate at higher frequencies. Figure 5 shows the transmission of the single slit as a
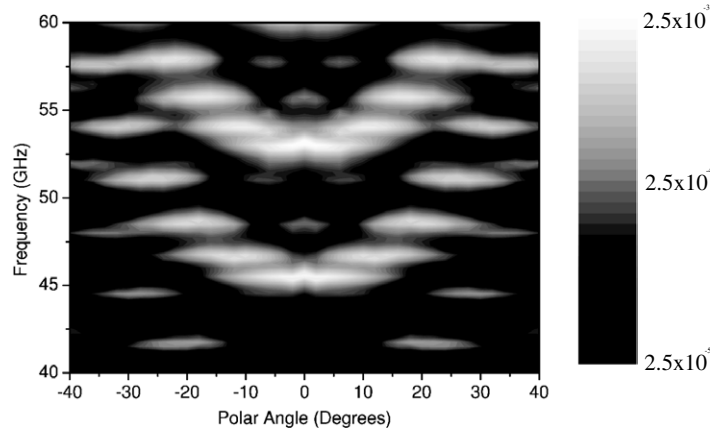
Figure 6. Angle scan FEM data of the structure shown in figure 1. Compares to data in figure 5(d). Intensity plotted on a logarithmic scale.

function of angle for slit lengths of 200, 100, 40, 25 and 8 mm over an incident angle range of $-40 < \theta < +40°$.

A vertical cross-section through the centre of each of the figures represents the resonant transmission of the slit when illuminated at normal incidence. In figures 5(a)–(d), modes $N = 6$ and 7 are shown ($\sim$46 and $\sim$54 GHz respectively) and in figure 5(e) the rise in resonant frequency is so great that the $N = 5$ mode appears at $\sim$42 GHz. Figure 5(e) also shows that the resonant peaks are roughly equally spaced in frequency, another prediction of equation (3). However, the most striking change in the transmission of the slit is as a function of slit length. The longest slit, which in relation to the wavelength of this frequency range could approximate to infinity (200 mm cf $\sim$6 mm), shows a smoothly rising frequency response for each resonant mode. This change in resonant frequency is due to the conservation of tangential photon momentum along the x-axis, whilst still maintaining the resonance in the z-direction (fixed by the resonant cavity depth, t). Thus, the resonant frequencies for an infinitely long slit, for incident angle θ, are approximated by:

$$f_N \approx \frac{c}{2\pi} \left[\left(\frac{N\pi}{t} \right)^2 + k_0^2 \sin^2 \theta \right]^{1/2}. \tag{4}$$

It is interesting that this condition is still true when the slit length is significantly reduced, as shown in figure 5(c; dashed white line), in which the slit length is only 40 mm. This indicates that the response of the slit is same as it is when the slit is infinitely long; however, the presence of the metal spacers constricts the length forcing the component of momentum along the length to be quantized. This quantization corresponds to higher-order resonant modes existing along the x-axis of the slit. To show this, the computer model is first compared with the data over the same range of angle, not just the normal incidence of figure 2, so that the resonant fields may be displayed with confidence.

To explore the field profiles of the resonance off normal incidence, the computer model is used to generate the grey scale shown in figure 6. It corresponds to a slit of length 25 mm, width 80 μm and depth 19.58 mm. The experimental data that this model replicates is shown in
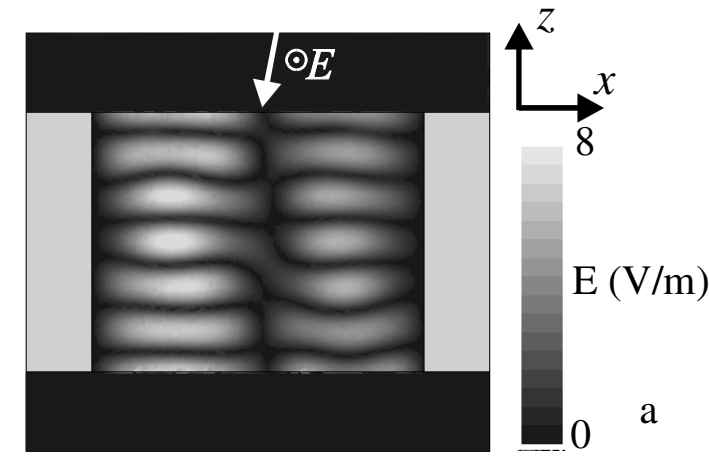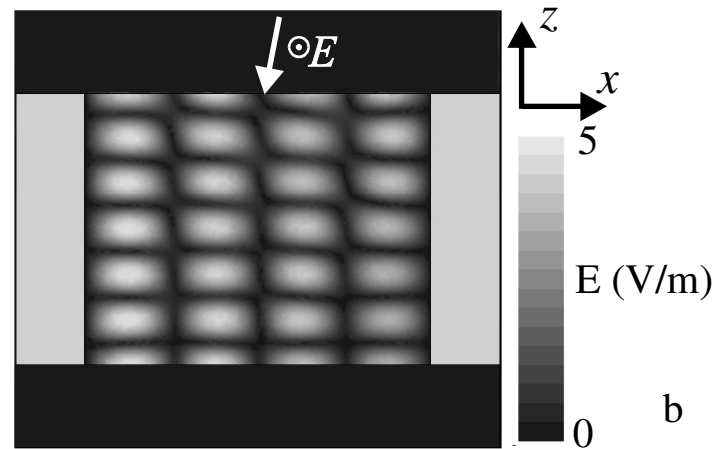
Fig.7a

Fig.7b

Figure 7. (a) Time-averaged electric field magnitude of the resonance at $13°$, $46.8\,\text{GHz}$ in figure (5); mode shown is $N = 6$ and $M = 2$. (b) Time-averaged electric fields of the resonance at $25°$, $51.2\,\text{GHz}$; mode shown is $N = 6$ and $M = 4$. Incident microwave beam and axes are shown, corresponding to the computer model. Incident electric field magnitude $= 1\,\text{V}\,\text{m}^{-1}$.

figure 5(d). The agreement between the two figures clearly shows that the computer model is indeed accurate enough to allow us to confidently explore the resonant fields.

Figures 7(a) and (b) show the resonant electric fields inside the slit for subbands recorded at $\sim 13°$, $\sim 46.8\,\text{GHz}$ (figure 7(a)) and $\sim 25°$, $\sim 51.2\,\text{GHz}$ (figure 7(b)) in the computer generated slit response in figure 6 which correspond to the $N = 6$, $M = 2$ and $N = 6$, $M = 4$ modes respectively. Again the different character of the orthogonal standing wave resonances are apparent, perhaps even more distinctly given the higher order resonances along each axis. The strength of the fields within the slits at these angles is shown to be much reduced from that of the modes at normal incidence. This is expected as the effective area of the slit presented

Institute *of* **Physics** Φ DEUTSCHE PHYSIKALISCHE GESELLSCHAFT

to the incident beam is reduced due to the higher incident angle and the coupling condition is also changed. The increased angle of incidence also accounts for the uneven distribution of the maxima of the resonant mode.

The computer modelled grey scales show further subtle resonant features which are not seen in the data as they are overwhelmed by interference. At $0°$, ~ 48.8 GHz, another faint resonant mode is visible in the computed response of figure 6. This is formed by weak coupling of the microwaves to the $N = 6$, $M = 3$ resonant mode at normal incidence. This is possible as the coupling conditions for the odd modes require that the field profile is symmetric at the slit ends. A normally incident plane wave is in phase across the entire surface, ideal for coupling to symmetric ($M = $ odd) modes, but not anti-symmetric ($M = $ even) ones. To couple to the even modes, a variation of phase is required across the length of the slit; this is provided by rotating the incident microwave beam off normal in the x–z-plane. As an example of this, a further faint sub-band is seen at the same angle of incidence as the $N = 6$, $M = 2$ mode but at higher frequency ~ 51.2 GHz. This is the result of weak coupling into the higher $M = 4$ resonant order mode.

3. Summary

The resonant transmission of a single subwavelength slit of finite length is explored in detail. It has been shown that as the slit length is reduced the frequency of each of the transmitted resonant modes rises monotonically. This increase, predicted by equation (3), arises from resonant field quantization in two orthogonal directions within the slit, as opposed to the quantization in the single direction of the long single slit. However, the resonant frequencies are shown to be below the simple approximation, due to the open ends of the slit. Nevertheless, there is excellent agreement of the experimental data with the FEM model which has allowed the reproduction of the slit's internal fields in detail. The magnetic fields at resonance have been shown to be temporally and spatially out of phase along the z-axis of the slit just as in an infinitely long slit. By contrast, the magnetic fields along the x-axis of the slit are in phase spatially, forced into this profile by the presence of the metal spacers. Increasing the angle of incidence of the microwaves causes the resonant frequency of each mode to increase as though the slit is infinite in length. However, the presence of the metal foil which bounds the slit causes a quantization of the main resonant band as higher-order modes are created along the length of the slit. These have been shown to have an uneven distribution of magnitude within the slit, a consequence of the angle of incidence. By investigating the resonant transmission of the single finite length subwavelength slit in deep metal plate, this work presents a useful insight into the transmission character of an intermediate structure between that of the single subwavelength hole and the long subwavelength slit, and hence a greater understanding of the differences between the two regimes.

Institute *of* **Physics** ⏀ DEUTSCHE PHYSIKALISCHE GESELLSCHAFT

References

[1] Ebbesen T W, Lezec H J, Ghaemi H F, Thio T and Wolff P A 1998 *Nature (London)* **391** 667
[2] Bethe H A 1944 *Phys. Rev.* **66** 163
[3] Schroter U and Heitmann D 1998 *Phys. Rev.* B **58** 15419
[4] Porto J A, Garcia-Vidal F J and Pendry J B 1999 *Phys. Rev. Lett.* **83** 2845
[5] Astilean S, Lalanne Ph and Palamaru M 2000 *Opt. Commun.* **175** 265
[6] Collin S, Pardo F, Teissier T and Pelouard J-L 2002 *J. Opt. A: Pure Appl. Opt.* **4** 154
[7] Went H E, Hibbins A P, Sambles J R, Lawrence C R and Crick A P 2000 *Appl. Phys. Lett.* **77** 2789
[8] Takakura Y 2001 *Phys. Rev. Lett.* **86** 5601
[9] Yang F and Sambles J R 2002 *Phys. Rev. Lett.* **89** 063901
[10] Suckling J R, Hibbins A P, Lockyear M J, Sambles J R and Lawrence C R 2004 *Phys. Rev. Lett.* **92** 147401
[11] Degiron A, Lezec H J, Yamamoto N and Ebbesen T 2004 *Opt. Commun.* **239** 61
[12] Garcia-Vidal F J, Moreno E, Porto J A and Martin-Moreno L 2005 *Phys. Rev. Lett.* **95** 103901
[13] Reitz J R, Milford F J and Christy R W 1993 *Foundations of Electromagnetic Theory* 4th edn (Reading, MA: Addison-Wesley)